Published in final edited form as:
*Eur J Nucl Med Mol Imaging*. 2011 November ; 38(11): 2066–2076. doi:10.1007/s00259-011-1886-x.

# In vivo near-infrared fluorescence imaging of CD105 expression during tumor angiogenesis

**Yunan Yang**[1,2,6], **Yin Zhang**[3,6], **Hao Hong**[1], **Glenn Liu**[4], **Bryan R. Leigh**[5], and **Weibo Cai**[1,3,4,*]

[1]Department of Radiology, University of Wisconsin - Madison, Madison, WI, USA

[2]Department of Ultrasound, Xinqiao Hospital, Third Military Medical University, Chongqing 400037, P. R. China

[3]Department of Medical Physics, University of Wisconsin - Madison, Madison, WI, USA

[4]University of Wisconsin Carbone Cancer Center, Madison, WI, USA

[5]TRACON Pharmaceuticals, Inc., San Diego, CA, USA

## Abstract

**Objectives—**Angiogenesis is an indispensable process during tumor development. The currently accepted standard method for quantifying tumor angiogenesis is to assess microvessel density (MVD) based on CD105 staining, which is an independent prognostic factor for survival in patients of most solid tumor types. The goal of this study is to evaluate tumor angiogenesis in a mouse model by near-infrared fluorescence (NIRF) imaging of CD105 expression.

**Methods—**TRC105, a human/murine chimeric anti-CD105 monoclonal antibody, was conjugated to a NIRF dye (IRDye 800CW; Ex: 778 nm; Em: 806 nm). FACS analysis and microscopy studies were performed to compare the CD105 binding affinity of TRC105 and 800CW-TRC105. In vivo/ex vivo NIRF imaging, blocking studies, and ex vivo histology were performed on 4T1 murine breast tumor-bearing mice to evaluate the ability of 800CW-TRC105 to target tumor angiogenesis. Another chimeric antibody, Cetuximab, was used as an isotype-matched control.

**Results—**FACS analysis of HUVECs revealed no difference in CD105 binding affinity between TRC105 and 800CW-TRC105, which was further validated by fluorescence microscopy. 800CW conjugation of TRC105 was achieved in excellent yield (> 85%), with an average of 0.4 800CW molecules per TRC105. Serial NIRF imaging after intravenous injection of 800CW-TRC105 revealed that the 4T1 tumor could be clearly visualized as early as 30 minutes post-injection. Quantitative region-of-interest (ROI) analysis showed that the tumor uptake peaked at about 16 h post-injection. Based on ex vivo NIRF imaging at 48 h post-injection, tumor-uptake of 800CW-TRC105 was higher than most organs thus providing excellent tumor contrast. Blocking experiments, control studies with 800CW-Cetuximab and 800CW, as well as ex vivo histology all confirmed the in vivo target specificity of 800CW-TRC105.

**Conclusions—**This is the first successful NIRF imaging study of CD105 expression in vivo. Fast, prominent, persistent, and CD105-specific uptake of the probe during tumor angiogenesis was observed in mouse models. 800CW-TRC105 may be used in the clinic for imaging tumor

Requests for reprints: Weibo Cai, PhD, Departments of Radiology and Medical Physics, School of Medicine and Public Health, University of Wisconsin – Madison, 1111 Highland Ave, Room 7137, Madison, WI 53705-2275, USA, wcai@uwhealth.org; Phone: 608-262-1749; Fax: 608- 265-0614.

[6]Contributed equally to this work

**Conflicts of interest**

BRL is an employee of TRACON Pharmaceuticals, Inc. The other authors declare that they have no conflict of interest.

angiogenesis within the lesions close to the skin surface, tissues accessible by endoscopy, or during image-guided surgery.

**Keywords**

CD105/endoglin; Near-infrared fluorescence (NIRF) imaging; Tumor angiogenesis; Monoclonal antibody (mAb); TRC105; Breast cancer

## Introduction

Most solid tumor growth depends on angiogenesis, the formation of new blood vessels [1]. One of the most suitable molecular markers for evaluating tumor angiogenesis is CD105 (endoglin) [2, 3]. As a disulfide-linked homodimeric transmembrane protein with a molecular weight of 180 kDa, CD105 is composed of short intracellular and transmembrane domains and a large extracellular region [4, 5]. Studies have revealed that CD105 is overexpressed on vascular endothelial cells of tissues undergoing angiogenesis (e.g. tumors or regenerating/inflamed tissues) [6–8], and CD105 expression level in the endothelia within neoplastic tissues correlates with the proliferation rate of endothelial cells [7, 8]. In addition, high CD105 expression also correlates with poor prognosis in more than 10 solid tumor types [9–11]. These findings support the role of CD105 as an optimal marker for tumor angiogenesis, underscoring its emerging clinical potential as a prognostic, diagnostic, and therapeutic target in the fight against cancer [12].

Non-invasive imaging of CD105 expression could represent a new paradigm for the assessment of anti-angiogenic therapeutics, thereby facilitating the understanding of the role and expression profile of CD105 in angiogenesis-related diseases [11, 13, 14]. To date, molecular imaging techniques that have targeted CD105 include molecular magnetic resonance imaging [15], ultrasound [16–18], single-photon emission computed tomography [8, 19, 20], and positron emission tomography (PET) [21]. Another study also investigated a $^{177}$Lu-labeled anti-CD105 antibody for potential radioimmunotherapy applications [22]. All of these studies are based on conjugating various imaging or therapeutic labels (e.g., radioisotopes such as $^{111}$In/$^{99m}$Tc/$^{125}$I/$^{177}$Lu/$^{64}$Cu, Gd-DTPA liposomes, or microbubbles) to anti-CD105 monoclonal antibodies (e.g. MAEND3, E9, MJ7/18, and TRC105) [14].

Optical imaging is an inexpensive and convenient method suitable primarily for small animal studies. The main drawback of fluorescence imaging is that it is typically not quantitative and the image information is surface-weighted due to tissue absorption and scattering [23]. For in vivo applications, imaging in the near-infrared (NIR; 700 - 900 nm) region, where the absorbance spectra for all biomolecules reach minima thus providing a clear optical window [24], can provide better opportunities for visualizing tumor angiogenesis in both small animal models and various clinical scenarios. In addition to better tissue penetration of light, there is also significantly less background signal due to tissue autofluorescence in the NIR window. To the best of our knowledge, NIR fluorescence (NIRF) imaging of CD105 expression has not been reported to date.

TRC105 is a human/murine chimeric IgG1 monoclonal antibody which binds to both human and murine CD105 (with higher affinity to the former). The murine parent antibody of TRC105 has been shown to induce apoptosis of human endothelial cells [25], mediate TGF-β-dependent inhibition of human endothelium [26], and inhibit tumor growth in mice [27]. TRC105 has a very high avidity (with a $K_D$ of 2 ng/mL) for human CD105 and is currently in a multicenter Phase 1 first-in-human dose-escalation trial in the United States [28]. Multiple Phase 2 therapy trials are planned or underway in patients with various solid tumor types. In this study, we conjugated TRC105 with IRDye 800CW (Ex: 778 nm; Em: 806 nm)

and investigated 800CW-TRC105 both in vitro and in vivo for NIRF imaging of tumor angiogenesis.

## Materials and methods

### Reagents

TRC105 was provided by TRACON pharmaceuticals Inc. (San Diego, CA). Cetuximab (a human/murine chimeric IgG1 monoclonal antibody that binds to human epidermal growth factor receptor with no cross-reaction with murine tissues [21, 29]) was from Bristol-Meyers Squibb Company (Princeton, NJ). AlexaFluor488- and Cy3-labeled secondary antibodies (Jackson Immunoresearch Laboratories, Inc., West Grove, CA), IRDye 800CW-NHS ester (LI-COR Biosciences Co., Lincoln, NE), PD-10 desalting columns (GE Healthcare, Piscataway, NJ) were acquired from commercial sources. All other chemicals used in this study were purchased from Sigma-Aldrich (St. Louis, MO).

### Cell lines and animal model

4T1 murine breast cancer, MCF-7 human breast cancer, and human umbilical vein endothelial cells (HUVECs) were purchased from the American Type Culture Collection (ATCC, Manassas, VA). 4T1 and MCF-7 cells were cultured in RPMI 1640 medium (Invitrogen, Carlsbad, CA) with 10% fetal bovine serum and incubated at 37 °C with 5% $CO_2$. HUVECs were cultured in M-200 medium (Invitrogen, Carlsbad, CA) with 1× low serum growth supplement (Cascade Biologics, Portland, OR) and incubated at 37 °C with 5% $CO_2$. Cells were used for in vitro and in vivo experiments when they reached ~80% confluence.

All animal studies were conducted under a protocol approved by the University of Wisconsin Institutional Animal Care and Use Committee. For the 4T1 tumor model, four- to five-week-old female Balb/c mice were purchased from Harlan (Indianapolis, IN) and tumors were established by subcutaneously injecting $2 \times 10^6$ cells suspended in 100 μL of 1:1 mixture of RPMI 1640 and Matrigel (BD Biosciences, Franklin lakes, NJ) into the front flank of mice [30]. The tumor sizes were monitored every other day and the animals were subjected to in vivo experiments when the diameter of tumors reached 6–8mm (about 7–10 days after inoculation).

### Conjugation of 800CW to antibodies

A molar ratio of 1:1 was used for the reactions between 800CW-NHS and TRC105 or Cetuximab, to avoid self-quenching of the fluorescence signal caused by multiple 800CW molecules on the same antibody. 800CW-NHS was dissolved in DMSO to form a stock solution of 25 mg/mL. The pH value of the reaction mixtures was adjusted to 8.5 with 0.1 M NaOH. After continuously stirring the reaction mixture at room temperature (RT) for 2 h, 800CW-TRC105 and 800CW-Cetuximab were purified with PD-10 columns using phosphate-buffered saline (PBS) as the mobile phase. The final concentrations of 800CW-TRC105 and 800CW-Cetuximab were measured based on UV absorbance at 280 nm using known concentrations of unconjugated TRC105 or Cetuximab as the standard, with minor corrections to take into account the absorbance of 800CW on the antibodies (i.e. absorbance of 800CW-antibody conjugate at 280 nm was ~3% higher than the antibody itself). The purified 800CW-TRC105 and 800CW-Cetuximab were passed through 0.2 μm syringe filters and stored in the dark at 4 °C for future experiments.

### Flow cytometry and microscopy

The immunoreactivity of TRC105 and 800CW-TRC105 to HUVECs (high CD105 expression [8, 31]) and MCF-7 cells (CD105-negative [8]) was evaluated by flow cytometry

analysis. Briefly, cells were harvested and suspended in cold PBS with 2% bovine serum albumin (BSA) at a concentration of $5 \times 10^6$ cells/mL. The cells were incubated with TRC105 or 800CW-TRC105 (1 or 5 μg/mL for HUVECs and 15 μg/mL for MCF-7 cells) for 30 min at RT, washed three times with cold PBS, and centrifuged at 1,000 rpm for 5 min. The cells were then incubated with AlexaFluor488-labeled goat anti-human IgG for 30 min at RT. Afterwards, the cells were washed and analyzed by flow cytometry using a BD FACSCalibur 4-color analysis cytometer equipped with 488nm and 633nm lasers (Becton-Dickinson, San Jose, CA) and FlowJo analysis software (Tree Star, Inc., Ashland, OR). HUVECs were also incubated with TRC105 or 800CW-TRC105 (2 μg/mL) and then examined under a Nikon Eclipse Ti microscope to further validate the FACS results.

### In vivo and ex vivo NIRF imaging

For all imaging studies, 800CW-labeled antibodies or 800CW carboxylate were injected intravenously through the tail vein at a dose of 300 picomole (pmol) of 800CW per mouse. The hair on the back of each mouse was removed before imaging studies. Under anesthesia with 2% isoflurane in $O_2$, the mice were imaged at multiple time points post injection (p.i.) in a Pearl Impulse scanner (LI-COR, Inc., Lincoln, NE) using the 800/white channels. To confirm the CD105 specificity of 800CW-TRC105 in vivo, a separate group of three mice were each pre-injected with 2 mg of TRC105 before 800CW-TRC105 administration (i.e. blocking). After the last scans at 48 h p.i., mice were euthanized. Blood, 4T1 tumor, and major organs/tissues were harvested and imaged again ex vivo to validate the in vivo findings.

Longitudinal images for each mouse were normalized with common minimum and maximum values. Using the vendor software, regions-of-interest (ROIs) were drawn on the 4T1 tumors and various other organs of interest. The average signal intensity (in the unit of counts/s/$mm^2$) within the ROI was used for subsequent quantitative analysis. The fluorescence intensity of the 4T1 tumor based on in vivo NIRF imaging was presented as mean ± SD (n = 3).

### Immunofluorescence staining

Frozen tissue slices of 5 μm thickness were fixed with cold acetone for 10 min and dried in the air for 30 min. After rinsing with PBS and blocking with 10% donkey serum for 30 min at RT, the slices were incubated with TRC105 (2 μg/mL) for 1 h at 4 °C and visualized using AlexaFluor488-labeled goat anti-human secondary antibody. The tissue slices were also stained for endothelial marker CD31 as described previously [32]. After washing with PBS, the tissue slices were incubated with rat anti-mouse CD31 antibody (2 μg/mL) for 1 h, followed by Cy3-labeled donkey anti-rat IgG for 30 min. All images were taken with a Nikon Eclipse Ti microscope.

### Measurement of circulation half-life

TRC105 and Cetuximab were each conjugated to 1,4,7,10-tetraazacyclododecane-1,4,7,10-tetraacetic acid (DOTA) and labeled with $^{64}Cu$ [21]. Two groups of 4T1 tumor-bearing mice (n = 3) were each injected with 7.4–12.95 MBq of $^{64}Cu$-DOTA-TRC105 or $^{64}Cu$-DOTA-Cetuximab. Approximately 5–40 μL of blood was taken from the tail vein of each mouse at different time points p.i. The radioactivity in the blood samples was measured using a γ-counter and calculated as percentage of injected dose per gram of tissue (%ID/g). The values of blood circulation half-life were calculated based on first-order exponential decay fits.

### Statistical analysis

Quantitative data were expressed as mean ± SD. Means were compared using Students' *t* test. P values < 0.05 were considered statistically significant.

## Results

### Comparison of 800CW-TRC105 and TRC105 in vitro

800CW conjugation of TRC105 or Cetuximab was achieved in excellent yield (> 85%), with an average of 0.4 800CW dye per antibody molecule (to avoid self-quenching of the dye). As shown in Fig. 1, 800CW conjugation of TRC105 did not affect its CD105 binding affinity, as evidenced by both FACS analysis and fluorescence microscopy. In FACS analysis of HUVECs (which express a high level of CD105), there was no observable difference between TRC105 and 800CW-TRC105 at 1 μg/mL or 5 μg/mL concentration (Fig. 1a). On the other hand, neither TRC105 nor 800CW-TRC105 bound to CD105-negative MCF-7 cells even at a much higher concentration of 15 μg/mL (Fig. 1a). Fluorescence microscopy studies of HUVECs also revealed no significant difference between TRC105 and 800CW-TRC105 (Fig. 1b). Taken together, these in vitro studies confirmed that 800CW conjugation did not affect the antigen binding affinity/specificity of TRC105.

### In vivo NIRF imaging

After intravenous injection of the NIRF agents (800CW-TRC105, pre-injection of a blocking dose of 2 mg of TRC105 before 800CW-TRC105, 800CW carboxylate, or 800CW-Cetuximab), 4T1 tumor-bearing mice were scanned at 0.5, 1, 2, 4, 16, 24, and 48 h p.i. and representative images from each group are shown in Fig. 2. Excellent tumor contrast was observed for 800CW-TRC105 as early as 0.5 h p.i. Subsequently, the tumor uptake continued to increase and plateaued at 16 h p.i., suggesting specific interaction between the antibody and its antigen. Quantitative ROI analysis yielded average tumor signal intensity of $1.91\times10^4 \pm 1.10\times10^4$, $1.98\times10^4 \pm 0.40\times10^4$, $2.63\times10^4 \pm 0.76\times10^4$, $3.70\times10^4 \pm 0.52\times10^4$, $5.11\times10^4 \pm 1.05\times10^4$, $4.68\times10^4 \pm 1.16\times10^4$, and $4.94\times10^4 \pm 0.98\times10^4$ counts/s/mm$^2$ at 0.5, 1, 2, 4, 16, 24, and 48 h p.i., respectively (Fig. 3a). Pre-injection of 2 mg of TRC105 per mouse before 800CW-TRC105 administration significantly reduced the tumor signal intensity to $0.73\times10^4 \pm 0.15\times10^4$, $0.94\times10^4 \pm 0.52\times10^4$, $1.00\times10^4 \pm 0.34\times10^4$, $1.24\times10^4 \pm 0.47\times10^4$, $1.58\times10^4 \pm 0.67\times10^4$, $1.61\times10^4 \pm 0.40\times10^4$, and $1.27\times10^4 \pm 0.35\times10^4$ counts/s/mm$^2$ at 0.5, 1, 2, 4, 16, 24, and 48 h p.i., respectively (Fig. 2 & 3a; $P < 0.05$ for all time points starting from 1 h p.i. when compared to 800CW-TRC105). Successful blocking experiments with TRC105 confirmed the CD105 specificity of 800CW-TRC105 in vivo.

Certain fluorescent dyes can have non-specific accumulation in tumors without conjugation to any targeting ligands [33]. Therefore, a group of mice were injected with 800CW carboxylate (upon hydrolysis of 800CW-NHS ester) to investigate this aspect. It was found that 800CW distributes quite uniformly in mice at early time points with poor tumor contrast (Fig. 2). In addition, 800CW cleared quite rapidly from the mice through the renal pathway, with virtually undetectable signal after 4 h p.i. Quantitative ROI analysis yielded average tumor signal intensity of $6.28\times10^4 \pm 0.96\times10^4$, $5.99\times10^4 \pm 0.74\times10^4$, $4.36\times10^4 \pm 0.21\times10^4$, $1.19\times10^4 \pm 6.47\times10^2$, $2.02\times10^3 \pm 1.70\times10^2$, $1.74\times10^3 \pm 0.77\times10^2$, and $1.09\times10^3 \pm 1.06\times10^2$ counts/s/mm$^2$ at 0.5, 1, 2, 4, 16, 24, and 48 h p.i., respectively (Fig. 3a; $P < 0.05$ for all time points when compared to 800CW-TRC105). All these findings confirmed that the fluorescence signal in the 4T1 tumor originated from CD105-specific binding of 800CW-TRC105, with little to no contribution from the non-specific accumulation of free 800CW in the tumor.

To further investigate the CD105 specificity of 800CW-TRC105, 800CW-Cetuximab was used as an isotype-matched control. Both TRC105 and Cetuximab are human/murine chimeric IgG1 monoclonal antibody. Since Cetuximab does not cross-react with murine tissues, it serves as an excellent control for investigating the tumor uptake due to passive targeting only (i.e. the enhanced permeability and retention effect). As can be seen in Fig. 2&3a, the uptake of 800CW-Cetuximab is significantly lower than 800CW-TRC105 at early time points ($P < 0.05$ at 1 h p.i. and $P < 0.01$ at 2 h and 4 h p.i.). The tumor signal intensity of 800CW-Cetuximab continued to increase over the 48 h period, however, the absolute signal intensity was still lower than that of 800CW-TRC105 at late time points.

ROI analysis of mice injected with 800CW-Cetuximab yielded average tumor signal intensity of $0.68\times10^4 \pm 0.24\times10^4$, $0.79\times10^4 \pm 0.25\times10^4$, $1.29\times10^4 \pm 0.60\times10^4$, $1.69\times10^4 \pm 0.69\times10^4$, $4.00\times10^4 \pm 1.56\times10^4$, $4.23\times10^4 \pm 0.87\times10^4$, and $4.37\times10^4 \pm 0.78\times10^4$ counts/s/mm$^2$ at 0.5, 1, 2, 4, 16, 24, and 48 h p.i., respectively (Fig. 3a). Since the circulation half-life of Cetuximab in 4T1 tumor-bearing mice is significantly longer than that of TRC105 (11.5 h vs. 3.5 h; Fig. 3b&c), the passive uptake of 800CW-Cetuximab increased gradually over an extended time period while the CD105-specific tumor uptake of 800CW-TRC105 increased rather rapidly. Such findings warrant caution in future antibody-based imaging studies as even isotype-matched IgGs may have rather different pharmacokinetics in vivo.

## Ex vivo NIRF imaging

All mice were euthanized after the last NIRF scans at 48 p.i. The 4T1 tumor and major tissues were collected for ex vivo NIRF imaging, as well as histological examination as described below, and representative images are shown in Fig. 4a. Consistent with our previous findings of $^{64}$Cu-labeled TRC105 [21], the uptake of 800CW-TRC105 in the liver (mostly due to hepatic clearance) was also prominent. Nonetheless, the tumor signal was higher than all other organs in the mice, thus providing excellent tumor contrast. Besides the liver, the kidneys also had detectable fluorescence signal, which is likely due to the clearance of 800CW, formed after degradation of the 800CW-TRC105 conjugate inside the cells after CD105-mediated endocytosis. The fluorescence signal in all other tissues was very low.

For 800CW-Cetuximab, only the liver and tumor have significant fluorescence signal at 48 h p.i. based on ex vivo NIRF imaging. Very weak signal was detected in the tissues harvested from mice injected with 800CW, since the majority of the dye was cleared from the mouse body rather quickly. Reduction in tumor fluorescence signal of 800CW-TRC105 by pre-injection of TRC105 was also confirmed by ex vivo NIRF imaging. Based on quantitative ROI analysis, the tumor fluorescence signals from the three control groups were all lower than that of 800CW-TRC105 (Fig. 4b). Overall, ex vivo NIRF imaging corroborates the findings from in vivo NIRF imaging, indicating that small animal imaging studies in the NIR window can allow for relatively accurate quantification.

## Histology

Immunofluorescence CD105/CD31 co-staining of tissue slices revealed that CD105 expression in the 4T1 tumor was almost exclusively on the tumor vasculature, as evidenced by excellent co-localization of CD105 and CD31 staining and very weak signal on the 4T1 tumor cells (Fig. 5). It is worth pointing out that CD105 expression is only on actively proliferating tumor endothelial cells. Some of the mature vessels in the 4T1 tumor, visualized by CD31 staining, do not express significant level of CD105 (arrowheads in Fig. 5). CD105 staining of the liver, spleen, and muscle all gave very low signal, indicating that these tissues do not have a significant level of CD105 expression (Fig. 5). Therefore, uptake of 800CW-TRC105 in the liver was primarily not related to CD105 binding, and likely due

to reticuloendothelial system capture and hepatic clearance. Taken together, the ex vivo data corroborated the in vivo observations, which warrants further investigation of this NIRF agent for imaging of tumor angiogenesis.

## Discussion

Over the last decade, molecular imaging of angiogenesis has gained tremendous interest since angiogenesis is a fundamental process in both normal physiology and many disease processes such as tumor development and metastasis [1, 34]. Two of the most intensively studied angiogenesis-related targets are integrin $\alpha_v\beta_3$ and vascular endothelial growth factor receptors (VEGFRs). Several tracers targeting these two receptors are already in clinical investigation [35–37]. Besides these two widely explored targets, CD105 is another very important tumor angiogenesis-related target. In clinical practice, the currently accepted standard method for quantifying tumor angiogenesis is to assess microvessel density (MVD) by performing CD105 immunohistochemistry on tumor tissue, which is an independent prognostic factor for survival in patients with many types of solid tumors [11, 38, 39]. CD105 has the advantage of being selectively expressed on proliferating endothelial cells at significantly higher levels (up to $3 \times 10^6$ copies per cell) than other angiogenic targets like the VEGFRs (less than $0.2 \times 10^6$ copies per cell) [31]. Surprisingly, molecular imaging of CD105 has not been well-studied in the literature [13, 14].

Non-invasive imaging of CD105 expression has the potential to accelerate drug development by providing a reliable measure of angiogenesis in the entire body as an intact system, thereby facilitating individualized treatment monitoring and dose optimization in animal models, clinical trials, and ultimately in the day-to-day management of cancer patients. Therefore, the goal of this study was to develop a CD105-specific NIRF agent for non-invasive imaging of tumor angiogenesis. We have achieved this goal and investigated 800CW-TRC105 in vitro, in vivo, and ex vivo. The experimental setup in this study represents the “best-case scenario” for optical imaging in that: 1) the emission maximum of 800CW is 806 nm, which is in the optically clear NIR window; 2) the tumors were subcutaneously inoculated, thus tissue penetration is not a major issue; 3) the use of laser excitation gives stronger signal than other excitation sources; and 4) the mouse hair was removed before NIRF imaging and the skin color of the mouse is very light. In clinical settings, NIRF imaging can be used for imaging tissues close to the surface of the skin (e.g. breast imaging), tissues accessible by endoscopy (such as the esophagus and colon), and intraoperative visualization (typically image-guided surgery).

The rationale for choosing the 4T1 tumor model for this study is that the parent antibody of TRC105 (SN6j, a monoclonal antibody of murine origin which binds to CD105) has been shown to be effective as an anti-angiogenic agent in this model [27]. Further, 4T1 tumor has highly angiogenic tumor vasculature (Fig. 5) which is expected to provide sufficient target density for imaging applications. We realized that one major limitation of this model is that the tumor vasculature is of murine origin. TRC105 has significantly higher affinity to human CD105 than its murine homolog [40]. Thus, the 4T1 tumor model is not optimal for testing TRC105. For future investigation, the following strategies may be evaluated to better mimic the clinical situation: using transgenic mice with human tumor vasculature or testing an anti-CD105 antibody that binds with high affinity to murine CD105. Follow-up studies are currently underway. Nonetheless, excellent tumor contrast was achieved in this study, even at early time points. The higher avidity of this agent to human CD105 is expected to exhibit even better tumor targeting capability in human patients (e.g. image-guided tumor resection) than we see here in mouse models of cancer.

One interesting finding from this study was the difference between the pharmacokinetic and biodistribution patterns of 800CW-TRC105 and 800CW-Cetuximab. The tumor uptake of 800CW-TRC105 (due to specific TRC105-CD105 interaction) increased quite rapidly and plateaued while tumor uptake of 800CW-Cetuximab (due to passive targeting only) increased much more slowly. The circulation half-lives were very different for these two isotype-matched antibodies. In recent human studies, a surprisingly short circulation half-life for TRC105 was also observed in cancer patients [28]. At doses of 20 mg or less (0.3 mg/kg), TRC105 is only detectable in the blood for 4 h or less. The half-life at a dose of 700 mg (10 mg/kg) is less than 24 h (unpublished data). The half-life of TRC105 will be longer at higher doses once CD105 in the tumor vasculature is saturated and after the tumor bulk is reduced.

The working hypothesis for such findings is that CD105 is an intravascular target that is immediately available to TRC105 upon injection (unlike tumor targets that require an antibody to diffuse out of the circulation and into a tumor before it can bind to its target). Tumor endothelial cells express CD105 at high copy numbers, which serves as an intravascular CD105 sink that rapidly sequesters the TRC105. Since TRC105 inhibits angiogenesis, the tumor becomes more hypoxic thereby inducing more CD105 expression on previously quiescent endothelial cells, thus functioning as a nearly endless TRC105 sink. Another explanation for such an obvious difference between isotype-matched antibodies (both TRC105 and Cetuximab are human/murine chimeric IgG1 type) is the lack of cross-reactivity with murine tissues for Cetuximab, which leads to longer circulation half-life and slower clearance/sequestration than TRC105 (which cross-reacts with murine CD105 although with lower affinity than human CD105).

## Conclusion

We have successfully investigated 800CW-TRC105 in vitro and in vivo. Non-invasive NIRF imaging revealed fast, prominent, persistent, and CD105-specific uptake of 800CW-TRC105 in the 4T1 tumor which was further validated by various in vitro and ex vivo experiments. Since TRC105 is already in clinical investigation and its therapeutic efficacy has been shown in various animal tumor models and certain cancer patients, successful NIRF imaging of CD105 warrants future investigation of 800CW-TRC105, where it may be used in the clinic to guide surgical resection of tumors, to detect superficial lesions, as well as to delineate tumors accessible by endoscopy.

## Acknowledgments

This work is supported, in part, by the University of Wisconsin Carbone Cancer Center, NCRR 1UL1RR025011, a DOD BCRP Postdoctoral Fellowship, a Susan G. Komen Postdoctoral Fellowship, and a DOD PCRP IDEA Award.

## References

1. Folkman J. Angiogenesis in cancer, vascular, rheumatoid and other disease. Nat Med. 1995; 1:27–31. [PubMed: 7584949]
2. Fonsatti E, Del Vecchio L, Altomonte M, Sigalotti L, Nicotra MR, Coral S, et al. Endoglin: An accessory component of the TGF-beta-binding receptor-complex with diagnostic, prognostic, and bioimmunotherapeutic potential in human malignancies. J Cell Physiol. 2001; 188:1–7. [PubMed: 11382917]
3. Wang JM, Kumar S, Pye D, van Agthoven AJ, Krupinski J, Hunter RD. A monoclonal antibody detects heterogeneity in vascular endothelium of tumours and normal tissues. Int J Cancer. 1993; 54:363–70. [PubMed: 8509210]

4. Barbara NP, Wrana JL, Letarte M. Endoglin is an accessory protein that interacts with the signaling receptor complex of multiple members of the transforming growth factor-beta superfamily. J Biol Chem. 1999; 274:584–94. [PubMed: 9872992]
5. Gougos A, Letarte M. Primary structure of endoglin, an RGD-containing glycoprotein of human endothelial cells. J Biol Chem. 1990; 265:8361–4. [PubMed: 1692830]
6. Wikstrom P, Lissbrant IF, Stattin P, Egevad L, Bergh A. Endoglin (CD105) is expressed on immature blood vessels and is a marker for survival in prostate cancer. Prostate. 2002; 51:268–75. [PubMed: 11987155]
7. Burrows FJ, Derbyshire EJ, Tazzari PL, Amlot P, Gazdar AF, King SW, et al. Up-regulation of endoglin on vascular endothelial cells in human solid tumors: implications for diagnosis and therapy. Clin Cancer Res. 1995; 1:1623–34. [PubMed: 9815965]
8. Fonsatti E, Jekunen AP, Kairemo KJ, Coral S, Snellman M, Nicotra MR, et al. Endoglin is a suitable target for efficient imaging of solid tumors: in vivo evidence in a canine mammary carcinoma model. Clin Cancer Res. 2000; 6:2037–43. [PubMed: 10815930]
9. Dallas NA, Samuel S, Xia L, Fan F, Gray MJ, Lim SJ, et al. Endoglin (CD105): a marker of tumor vasculature and potential target for therapy. Clin Cancer Res. 2008; 14:1931–7. [PubMed: 18381930]
10. Kumar S, Ghellal A, Li C, Byrne G, Haboubi N, Wang JM, et al. Breast carcinoma: vascular density determined using CD105 antibody correlates with tumor prognosis. Cancer Res. 1999; 59:856–61. [PubMed: 10029075]
11. Fonsatti E, Nicolay HJ, Altomonte M, Covre A, Maio M. Targeting cancer vasculature via endoglin/CD105: a novel antibody-based diagnostic and therapeutic strategy in solid tumours. Cardiovasc Res. 2010; 86:12–9. [PubMed: 19812043]
12. Seon BK, Haba A, Matsuno F, Takahashi N, Tsujie M, She X, et al. Endoglin-targeted cancer therapy. Curr Drug Deliv. 2011; 8:135–43. [PubMed: 21034418]
13. Cai W, Rao J, Gambhir SS, Chen X. How molecular imaging is speeding up antiangiogenic drug development. Mol Cancer Ther. 2006; 5:2624–33. [PubMed: 17121909]
14. Zhang Y, Yang Y, Hong H, Cai W. Multimodality molecular imaging of CD105 (Endoglin) expression. Int J Clin Exp Med. 2011; 4:32–42. [PubMed: 21394284]
15. Zhang D, Feng XY, Henning TD, Wen L, Lu WY, Pan H, et al. MR imaging of tumor angiogenesis using sterically stabilized Gd-DTPA liposomes targeted to CD105. Eur J Radiol. 2009; 70:180–9. [PubMed: 18541399]
16. Korpanty G, Grayburn PA, Shohet RV, Brekken RA. Targeting vascular endothelium with avidin microbubbles. Ultrasound Med Biol. 2005; 31:1279–83. [PubMed: 16176794]
17. Korpanty G, Carbon JG, Grayburn PA, Fleming JB, Brekken RA. Monitoring response to anticancer therapy by targeting microbubbles to tumor vasculature. Clin Cancer Res. 2007; 13:323–30. [PubMed: 17200371]
18. Deshpande N, Ren Y, Foygel K, Rosenberg J, Willmann JK. Tumor angiogenic marker expression levels during tumor growth: longitudinal assessment with molecularly targeted microbubbles and US imaging. Radiology. 2011; 258:804–11. [PubMed: 21339349]
19. Bredow S, Lewin M, Hofmann B, Marecos E, Weissleder R. Imaging of tumour neovasculature by targeting the TGF-beta binding receptor endoglin. Eur J Cancer. 2000; 36:675–81. [PubMed: 10738134]
20. Costello B, Li C, Duff S, Butterworth D, Khan A, Perkins M, et al. Perfusion of $^{99m}$Tc-labeled CD105 Mab into kidneys from patients with renal carcinoma suggests that CD105 is a promising vascular target. Int J Cancer. 2004; 109:436–41. [PubMed: 14961584]
21. Hong H, Yang Y, Zhang Y, Engle JW, Barnhart TE, Nickles RJ, et al. Positron emission tomography imaging of CD105 expression during tumor angiogenesis. Eur J Nucl Med Mol Imaging. 2011 Epub.
22. Lee SY, Hong YD, Felipe PM, Pyun MS, Choi SJ. Radiolabeling of monoclonal anti-CD105 with $^{177}$Lu for potential use in radioimmunotherapy. Appl Radiat Isot. 2009; 67:1366–9. [PubMed: 19324561]
23. Massoud TF, Gambhir SS. Molecular imaging in living subjects: seeing fundamental biological processes in a new light. Genes Dev. 2003; 17:545–80. [PubMed: 12629038]

24. Cai W, Hsu AR, Li ZB, Chen X. Are quantum dots ready for *in vivo* imaging in human subjects? Nanoscale Res Lett. 2007; 2:265–81. [PubMed: 21394238]
25. Tsujie M, Tsujie T, Toi H, Uneda S, Shiozaki K, Tsai H, et al. Anti-tumor activity of an anti-endoglin monoclonal antibody is enhanced in immunocompetent mice. Int J Cancer. 2008; 122:2266–73. [PubMed: 18224682]
26. She X, Matsuno F, Harada N, Tsai H, Seon BK. Synergy between anti-endoglin (CD105) monoclonal antibodies and TGF-beta in suppression of growth of human endothelial cells. Int J Cancer. 2004; 108:251–7. [PubMed: 14639611]
27. Tsujie M, Uneda S, Tsai H, Seon BK. Effective anti-angiogenic therapy of established tumors in mice by naked anti-human endoglin (CD105) antibody: differences in growth rate and therapeutic response between tumors growing at different sites. Int J Oncol. 2006; 29:1087–94. [PubMed: 17016638]
28. Mendelson DS, Gordon MS, Rosen LS, Hurwitz H, Wong MK, Adams BJ, et al. Phase I study of TRC105 (anti-CD105 [endoglin] antibody) therapy in patients with advanced refractory cancer. J Clin Oncol. 2010; 28:15s.
29. Vincenzi B, Zoccoli A, Pantano F, Venditti O, Galluzzo S. Cetuximab: from bench to bedside. Curr Cancer Drug Targets. 2010; 10:80–95. [PubMed: 20088790]
30. Wang H, Cai W, Chen K, Li ZB, Kashefi A, He L, et al. A new PET tracer specific for vascular endothelial growth factor receptor 2. Eur J Nucl Med Mol Imaging. 2007; 34:2001–10. [PubMed: 17694307]
31. Takahashi N, Haba A, Matsuno F, Seon BK. Antiangiogenic therapy of established tumors in human skin/severe combined immunodeficiency mouse chimeras by anti-endoglin (CD105) monoclonal antibodies, and synergy between anti-endoglin antibody and cyclophosphamide. Cancer Res. 2001; 61:7846–54. [PubMed: 11691802]
32. Cai W, Chen K, Mohamedali KA, Cao Q, Gambhir SS, Rosenblum MG, et al. PET of vascular endothelial growth factor receptor expression. J Nucl Med. 2006; 47:2048–56. [PubMed: 17138749]
33. Wu Y, Cai W, Chen X. Near-infrared fluorescence imaging of tumor integrin $\alpha_v\beta_3$ expression with Cy7-labeled RGD multimers. Mol Imaging Biol. 2006; 8:226–36. [PubMed: 16791749]
34. Carmeliet P. Angiogenesis in life, disease and medicine. Nature. 2005; 438:932–6. [PubMed: 16355210]
35. Cai W, Chen X. Multimodality imaging of vascular endothelial growth factor and vascular endothelial growth factor receptor expression. Front Biosci. 2007; 12:4267–79. [PubMed: 17485373]
36. Cai W, Chen X. Multimodality molecular imaging of tumor angiogenesis. J Nucl Med. 2008; 49 (Suppl 2):113S–28S. [PubMed: 18523069]
37. Cai W, Niu G, Chen X. Imaging of integrins as biomarkers for tumor angiogenesis. Curr Pharm Des. 2008; 14:2943–73. [PubMed: 18991712]
38. Duff SE, Li C, Garland JM, Kumar S. CD105 is important for angiogenesis: evidence and potential applications. FASEB J. 2003; 17:984–92. [PubMed: 12773481]
39. Fonsatti E, Sigalotti L, Arslan P, Altomonte M, Maio M. Emerging role of endoglin (CD105) as a marker of angiogenesis with clinical potential in human malignancies. Curr Cancer Drug Targets. 2003; 3:427–32. [PubMed: 14683500]
40. Matsuno F, Haruta Y, Kondo M, Tsai H, Barcos M, Seon BK. Induction of lasting complete regression of preformed distinct solid tumors by targeting the tumor vasculature using two new anti-endoglin monoclonal antibodies. Clin Cancer Res. 1999; 5:371–82. [PubMed: 10037187]

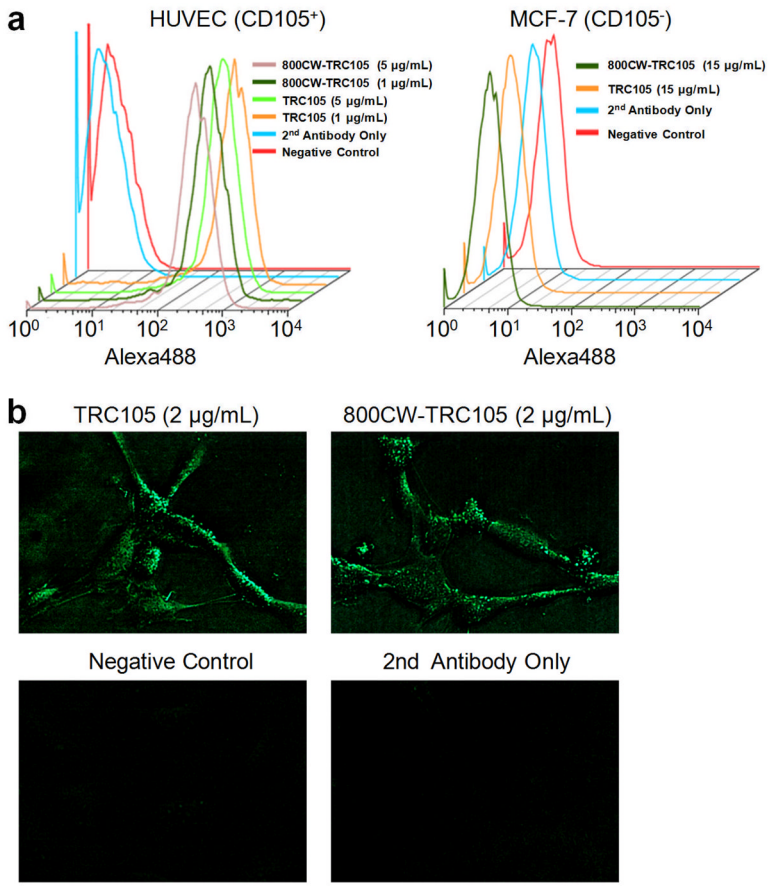


**Fig. 1.**

In vitro investigation of 800CW-TRC105. **a** Flow cytometry analysis of TRC105 and 800CW-TRC105 in HUVECs (CD105-positive) and MCF-7 (CD105-negative) cells at different concentrations. **b** Fluorescence microscopy images of HUVECs using either TRC105 or 800CW-TRC105 (2 μg/mL) as the primary antibody. Various control images are also shown.

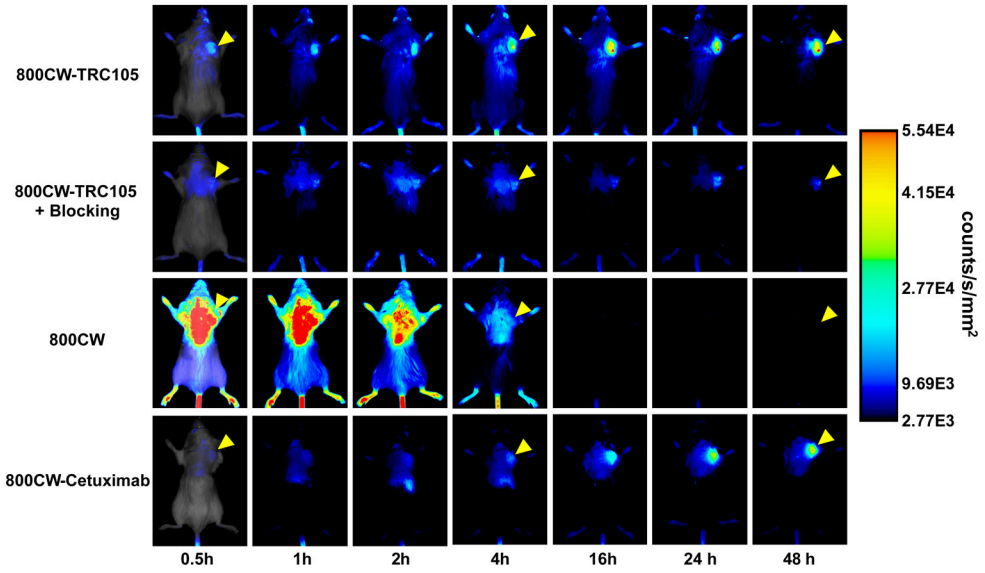


**Fig. 2.**

Serial near-infrared fluorescence imaging of 4T1 tumor-bearing mice after intravenous injection of 800CW-TRC105, pre-injection of a blocking dose of 2 mg of TRC105 before 800CW-TRC105 (denoted as “800CW-TRC105 + Blocking”), 800CW carboxylate, or 800CW-Cetuximab. The amount of 800CW injected into each mouse was 300 pmol and images are representative of a group of 3 mice each. All images were acquired under the same condition and displayed at the same scale. The first image in each row is a merged image of the fluorescence signal and a photo of the mouse, while subsequent images in each row are fluorescence images only. Arrowheads indicate the 4T1 tumors.

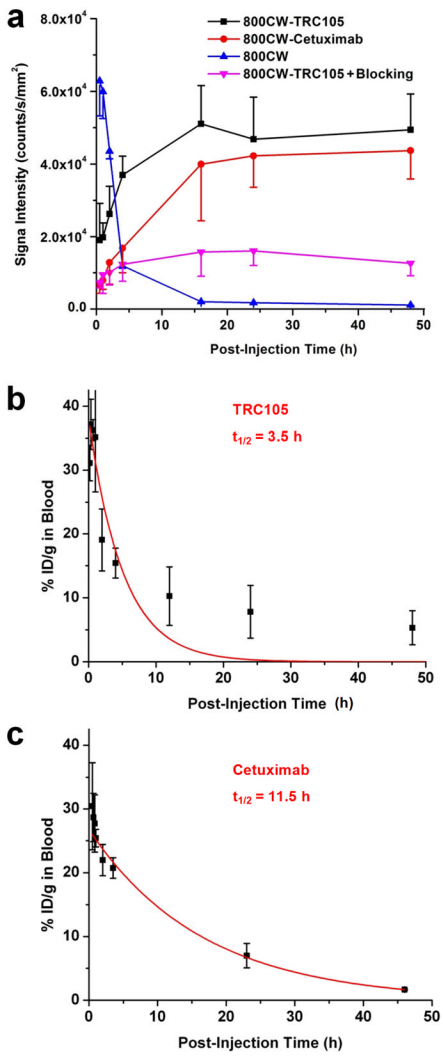


**Fig. 3.**

Quantitative analysis of the fluorescence data and measurement of circulation half-lives. **a** Average fluorescence signal intensity of the 4T1 tumor after injection of various 800CW-containing agents. Data were presented as mean ± SD (n = 3). When compared to the 800CW-TRC105 group, the P values were < 0.05 at all time points after 1 h post-injection (p.i.) for "800CW-TRC105 + Blocking", < 0.05 at all time points for 800CW, and < 0.05 at 1 h p.i. and < 0.01 at 2 and 4 h p.i. for 800CW-Cetuximab. **b** The circulation half-life of TRC105 in 4T1 tumor-bearing mice is 3.5 h based on first-order exponential decay fit (shown in red) of the blood radioactivity of intravenously injected $^{64}$Cu-DOTA-TRC105. **c** The circulation half-life of Cetuximab in 4T1 tumor-bearing mice is 11.5 h based on first-order exponential decay fit (shown in red) of the blood radioactivity of intravenously injected $^{64}$Cu-DOTA-Cetuximab.

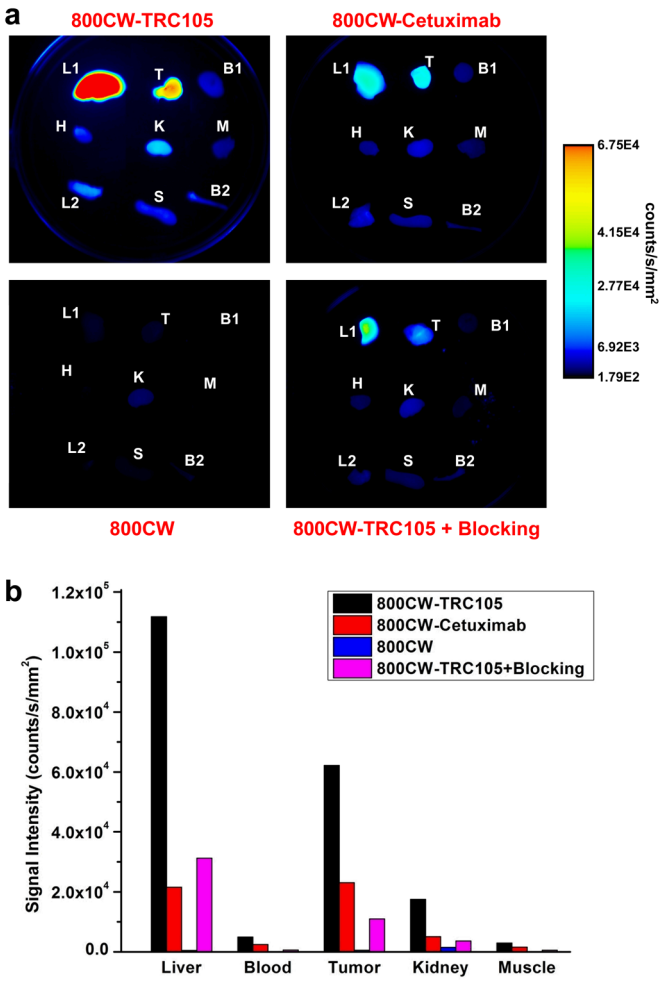


**Fig. 4.**

Ex vivo near-infrared fluorescence imaging. **a** Fluorescence images of the 4T1 tumor and major organs at 48 h post-injection of 800CW-TRC105, 800CW-Cetuximab, 800CW carboxylate, or 800CW-TRC105 + Blocking. The amount of 800CW injected into each mouse was 300 pmol and images are representative of a group of 3 mice each. All images were acquired under the same condition and displayed at the same scale. L1: liver, T: 4T1 tumor, B1: blood, H: heart, K: kidney, M: muscle, L2: lung, S: spleen, B2: bone. **b** Fluorescence signal intensity of the 4T1 tumor and certain major organs based on ex vivo near-infrared fluorescence imaging.

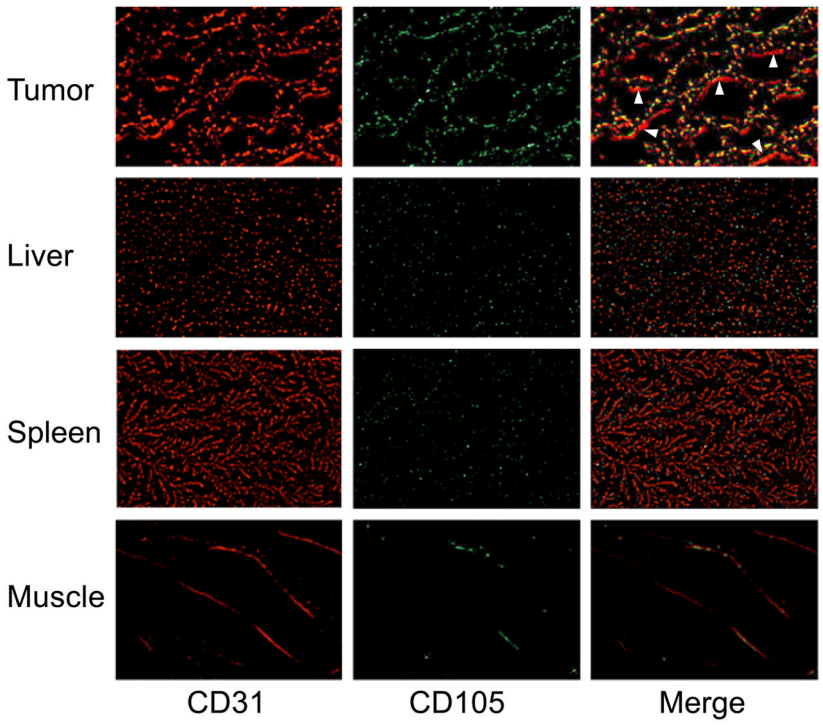


**Fig. 5.**

Immunofluorescence CD105 (green) and CD31 (red) double-staining of the 4T1 tumor, liver, spleen, and muscle tissue sections. Note that CD105 expression was high on newly formed blood vessels but not on mature vessels (visible by CD31 staining but not by CD105 staining; indicated by arrowheads). CD105 expression levels in the liver, spleen, and muscle are all much lower than in the tumor vessels. All images were acquired under the same condition and displayed at the same scale. Magnification: 200×.